

Cell lysis on a microfluidic CD (compact disc)

Jitae Kim,^a Seh Hee Jang,^b Guangyao Jia,^a Jim V. Zoval,^a Nancy A. Da Silva^b and Marc J. Madou^{*a}

^a Department of Mechanical and Aerospace Engineering, University of California, Irvine, CA 92697, USA. E-mail: mmadou@uci.edu; Fax: +1 949 824 8585; Tel: +1 949 824 6585

^b Department of Chemical Engineering and Materials Science, University of California, Irvine, CA 92697, USA

Received 23rd January 2004, Accepted 12th May 2004

First published as an Advance Article on the web 5th August 2004

Cell lysis was demonstrated on a microfluidic CD (Compact Disc) platform. In this purely mechanical lysis method, spherical particles (beads) in a lysis chamber microfabricated in a CD, cause disruption of mammalian (CHO-K1), bacterial (*Escherichia coli*), and yeast (*Saccharomyces cerevisiae*) cells. Interactions between beads and cells are generated in the rimming flow established inside a partially filled annular chamber in the CD rotating around a horizontal axis. To maximize bead–cell interactions in the lysis chamber, the CD was spun forward and backwards around this axis, using high acceleration for 5 to 7 min. Investigation on inter-particle forces (friction and collision) identified the following parameters; bead density, angular velocity, acceleration rate, and solid volume fraction as having the most significant contribution to cell lysis. Cell disruption efficiency was verified either through direct microscopic viewing or measurement of the DNA concentration after cell lysing. Lysis efficiency relative to a conventional lysis protocol was approximately 65%. In the long term, this work is geared towards CD based sample-to-answer nucleic acid analysis which will include cell lysis, DNA purification, DNA amplification, and DNA hybridization detection.

1 Introduction

Although extensive research on microfluidic devices¹ for biomedical and clinical diagnostic applications has been conducted in the past decade, a majority of the miniaturized devices has been limited to single purpose applications due to the complexity of integrating various microfluidic components into a single small unit. Compared to other microfluidic technologies^{2–4} for moving small amounts of fluid or suspended particles from site to site, a centrifuge-based system is well suited for various crucial microfluidic functions such as flow sequencing, mixing, capillary metering, and flow switching.^{5–7} Those functions can be implemented through the exploitation of the centrifugal and coriolis forces in combination with the capillary force and by relying on specific microfluidic designs. A polymer based microfluidic CD platform is a highly promising approach, not only for the integration of several microfluidic functions for diagnostic applications but also as a platform enabling the automated, multiple parallel processing needs in high-throughput screening (HTS). In this paper, we investigate the feasibility of mechanical cell lysis on a CD platform and compare its performance with a traditional lysis protocol.

There are many types of cell lysis methods used today that are based on mechanical,⁸ physico-chemical,⁹ chemical,¹⁰ and enzymatic¹⁰ principles. The most commonly used methods in biology research labs rely on chemical and enzymatic principles. The main drawbacks of those procedures include intensive labor, adulteration of cell lysate, and the need for additional purification steps. In order to minimize the required steps for cell lysis, a rapid and reagentless cell lysis method⁸ would be very useful, especially in sample preparation on a microfluidic platform such as the CD. Such an approach to lysis would also help avoid the storage of wet chemicals in micromachined chambers and the need for intensive mixing, both of which are generally considered difficult in the micro

domain. In the current work, a purely mechanical lysis method was investigated based on rapid granular shear flow^{11,12} in an annular chamber in a CD which spins about a horizontal axis of rotation alternating between the forward and reverse directions. When the CD is at rest, spherical particles, such as glass beads, in an aqueous medium containing cells to be disrupted, lie in a pool at the bottom of the chamber. However, during spinning all particles are dragged up by the surrounding medium and uniformly coat the outer wall of the chamber in response to both shear and centrifugal forces as shown in Fig. 1. This flow is often referred to as “rimming flow”.^{13,14} In order for a cell to be disrupted in a rapid granular flow, the cell should be brought into physical contact with the colliding particles. The bead interactions with the cells consist of two main types: impulsive contact (collision) due to the beads responding to the centrifugal field and sustained contact (friction) due to shearing.

We first discuss inter-particle forces involved in the rimming flow and identify those parameters that are expected to have the largest contribution to the inter-particle forces. The actual influence of these parameters on cell lysis is then verified

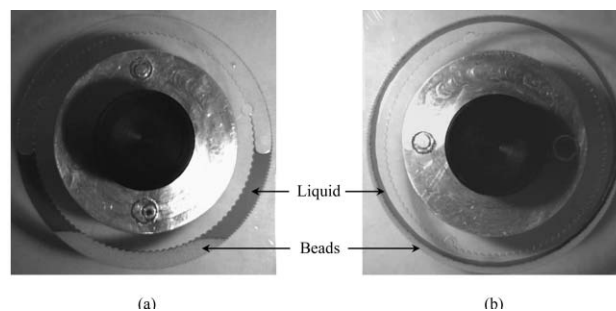


Fig. 1 Flow patterns for two rotational states of the CD (a) At rest: beads are sedimented at the bottom of the annular chamber (b) While spinning: two circumferential bands of beads and liquid are observed.

experimentally by microscopy or by measuring the double stranded DNA concentration extracted from the cells upon lysis.

II. Particle interactions (collision and friction between particles)

Rapid granular rimming flow in a horizontally rotating annular chamber features two types of particle interactions: collision and friction. In Fig. 2 we schematically depict these particle interactions generated during an acceleration period in a partially-filled lysis chamber. Collision occurs when suspended particles are forced to move outwards radially (vector $\mathbf{u}_s(t)$ in Fig. 2) responding to a centrifugal field and impact upon particles closer to the outer wall. Friction between particles is generated in the process of rearranging the impacting particles into a circumferential granule band along the outer wall. The impacting particles (see vector \mathbf{u}_1 in Fig. 2) travel slower than the particles close to the chamber outer wall (see vector \mathbf{u}_2 in Fig. 2) due to the evolving velocity profile associated with the growth of the boundary layer over the outer wall. Particles accumulated against the chamber outer wall move almost at the same tangential velocity ($U_T(t)$) as the outer chamber wall itself as they more or less stick to it. Thus it is the tangential velocity difference between impacting particles that leads to the friction between those particles.

Suspended particles describe a complete circle on a typical time scale of 0.05 s with the CD spinning at angular velocities ranging from 50–100 rev s^{-1} . This tangential velocity (vector $\mathbf{u}_T(t)$) is approximately three orders of magnitude larger than the particle velocity relative to the fluid in radially outward direction (vector $\mathbf{u}_s(t)$, *i.e.* the settling velocity). On the basis of this consideration, one can expect that the suspended particles, upon spinning the CD, uniformly coat the chamber wall while undergoing both collision and friction.

A. Friction

In granular suspension flows with a large shear rate, interaction of adjacent particles moving at different velocities leads to friction between those particles and consequently a repulsive pressure, P_r is induced. Bagnold¹⁵ empirically found that this repulsive pressure is proportional to the shear stress τ , and can be expressed as

$$P_r \propto \tau \propto \rho_p D_p^2 \gamma^2 f(C) \quad (1)$$

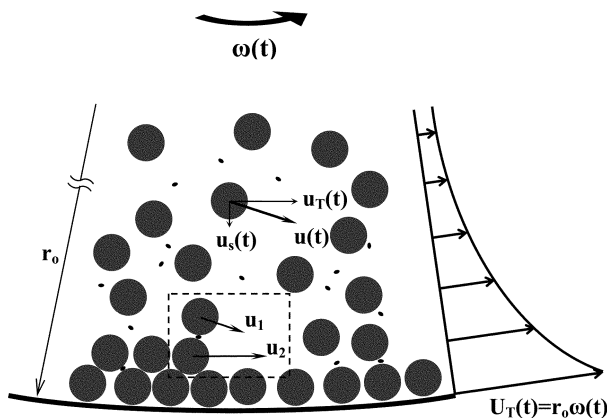


Fig. 2 Schematic representation of the particle interactions (collision and friction) that are generated during acceleration of a CD. A tangential velocity profile of fluid in the chamber is depicted on the right and varies with radial location and time. $\mathbf{u}_T(t)$ represents the tangential velocity of a particle in response to the shear flow. $\mathbf{u}_s(t)$ represents the settling velocity of the particle under a centrifugal field.

where ρ_p is particle density, D_p is particle diameter, γ is shear rate, and $f(C)$ is a function of the volumetric concentration of particles, C .

In eqn. (1), derived for steady state conditions, the inter-particle friction depends on the shear stress τ which is proportional to the square of the imposed shear rate γ (*i.e.*, dU/dy in plane Couette flow). This expression holds in the grain-inertia regime where a granular flow system is dominated by particle interactions. In the case of the CD, a shear rate is established in setting up a rimming flow in the annular chamber during acceleration. Therefore the inter-particle friction will vary with the acceleration rate of the CD since the shear rate depends on the acceleration. Accordingly, higher acceleration rate will lead to larger magnitude of frictional contact of particles.

B. Collision

Collision in this current context is the particle interaction occurring on the mound of particles at the outer wall, where radially moving particles, with an impact velocity (*i.e.*, a settling velocity) induced by the centrifugal force, smash against the particles on the mound (see also Fig. 2). Different from friction, described above, no tangential velocity gradient is involved in setting up the collision. Most of the theories on particle collisions^{16,17} in granular flow are based on models describing the individual collisions of spheres and adequately describe the average properties of the flow. However, the measurement of impact coefficients to test these theories is extremely challenging in the current application and is beyond the scope of this treatise. Instead, we have attempted to evaluate the parameters associated with a collisional particle pressure generated in the course of forming a granule suspension into the rimming flow in a rotating annular chamber in order to predict their contributions to the magnitude of the collision qualitatively.

In the work by Batchelor¹⁸ and Zenit *et al.*,¹⁹ a collisional particle pressure in a solid-liquid mixture is represented as

$$P_c = v \rho_p \bar{u}^2 F(v) \quad (2)$$

where v is the solid volume fraction (SVF), ρ_p is the particle density, and \bar{u} is the local mean particle velocity. Batchelor suggests the following solid volume fraction relationship

$$F(v) \approx \frac{v}{v_{cp}} \left(1 - \frac{v}{v_{cp}} \right) \quad (3)$$

where v_{cp} is the closed-packed solid fraction which is about 0.62 for a randomly packed bed of uniform sized particles. It is assumed that eqn. (2) is valid with $F(v)$ sufficiently far removed from the two extremes cases *i.e.*, with v approaching zero, and with v approaching the close-packed limit so that the equation applies only to a situation where most of particles are suspended in the chamber. Here, considering a solid-liquid suspension in a centrifugal field, it is appropriate that we substitute the settling velocity, $u_s(t)$ for the local mean particle velocity \bar{u} in eqn. (2). From a balance of the centrifugal, buoyancy²⁰ and drag forces, the motion of a spherical particle can be expressed as

$$m \frac{du_s}{dt} = m r \omega^2 - m \frac{\rho}{\rho_p} r \omega^2 - \frac{C_D}{2} u_s^2 A_p \rho \quad (4)$$

which can be rewritten as

$$\frac{du_s}{dt} = r \omega^2 \frac{\rho_p - \rho}{\rho_p} - \frac{C_D A_p \rho}{2m} u_s^2 \quad (5)$$

where ω is the angular frequency, r is the distance of the particle from the center of the disc, ρ is the liquid density, C_D is

the drag coefficient, and A_p is the projected area of the particle. As a particle travels, the drag quadratically increases with the velocity. Therefore, the particle acceleration quickly decreases and approaches zero. The particle then reaches a maximum constant velocity *i.e.*, the terminal settling velocity, which is calculated as

$$u_t = \sqrt{\frac{4r\omega^2 D_p(\rho_p - \rho)}{3C_D\rho}} \quad (6)$$

Since the particle Reynolds number, $Re_p = (D_p u_t \rho) / \eta$, is calculated to be slightly larger than 1 for the current experiments, falling into a transition region very close to Stokes regime, the drag coefficient²¹ is found as

$$C_D = \frac{24}{Re_p} + \frac{3}{\sqrt{Re_p}} + 0.34 \quad (7)$$

It is noted here that the eqn. (6) is only valid with the assumption that the particle reaches its maximum velocity relatively unimpeded by adjacent particles. For simplicity, we substitute the terminal settling velocity in eqn. (6) for the local mean particle velocity. Then, the collisional pressure in eqn. (2) can be rewritten as

$$P_c = \left\{ \frac{4rD_p}{3C_D} \right\} \left\{ \rho_p \left(\frac{\rho_p}{\rho} - 1 \right) \omega^2 v F(v) \right\} \quad (8)$$

Although we do not know the relative contributions of the repulsive and collisional particle pressures to cell lysis, we can, from the discussion about eqn. (1) and from eqn. (8), conclude that the important parameters for lysis are acceleration rate, particle density, angular velocity, solid volume fraction, and particle size. Concerning the volume fraction of particles, it plays a binary role in both the magnitude of particle interactions and the effective impact frequency, *i.e.*, the number of collision of particles in which a cell finds itself in-between. If only the collisional pressure in eqn. (2) is considered for the inter-particle force, the highest collisional pressure will lie at the SVF of 0.42 as shown in Fig. 3. In an effort to find an optimal SVF for our current CD design, SVF tests need to be carried out on the basis of the SVF of 0.42.

III Experimental setup and procedure

A Fabrication of PDMS CD

Polydimethylsiloxane (PDMS) has been widely used for the testing of microfluidic devices for biomedical applications because of its simple manufacturing process. A wide variety of PDMS structures can be achieved using standard soft lithography techniques.²² SU-8 photolithography is a good

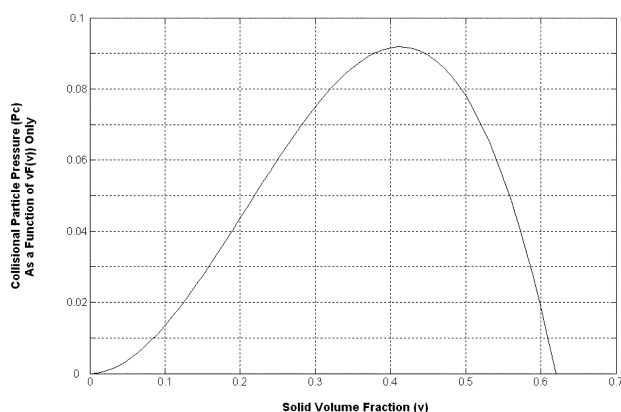


Fig. 3 Plot of a collisional particle pressure P_c with respect to solid volume fraction v .

choice for fabricating a master mold with very high features (say $> 500 \mu\text{m}$). Lorenz²³ demonstrated that structures more than $500 \mu\text{m}$ high could be achieved with a single-layer coating of SU-8 and even thicker structures could be made using multiple coatings. For the purpose of mechanical cell disruption, an ultra-thick SU-8 process was developed to fabricate a mold featuring extra high structures ($\sim 1 \text{ mm}$) so that sufficiently high lysing chambers could be formed in the PDMS for the interaction of beads.

A thick layer of SU-8 100 (MicroChem, MA) was spin-coated onto a 6 inch Si wafer (Addison Engineering, CA). Prebaking (90 min at 65°C and 120 min at 95°C) and postbaking (60 min at 65°C and 150 min at 95°C) processes were significantly elongated compared to the process data of Microchem²⁴ to achieve the desired master mold thickness. A higher exposure dose (2000 mJ cm^{-2}) was also applied for the same reason. The postbaking step is critical for good adhesion between the substrate and the crosslinked SU-8 structures. Insufficient postbaking and exposure would cause the structures to peel off during development. Another issue for thick SU-8 lithography is leveling. Adequate leveling of the SU-8 coated substrate was required during the baking steps to avoid significant thickness variation since the SU-8 reflows due to the lowered viscosity at the baking temperatures. The coated substrate was then cooled down gradually in an oven until its temperature decreased below 50°C . This step was intended to reduce residual stress in the pattern and at the Si/pattern interface. Development took about 50 min.

The PDMS precursor and curing agent (Dow Corning) were mixed thoroughly in a weight ratio of 10:1. After degassing the mixture in vacuum, it was poured and cured on the SU-8 master mold which has a rim fashioned around the substrate to contain the liquid PDMS. The rotating CD platform was completed by sandwiching the micromachined PDMS sheet between two polycarbonate discs. In Fig. 4(a) we show a CD with a typical annulus chamber designed for cell lysis. The wavy inner wall (see Fig. 4(b)) of the chamber is intended to assist in lifting up a solid-liquid suspension at the moment of spinning the CD (*i.e.*, little boundary layer growing). Many particles then stay longer around the inner wall so that we can take full advantage of the particle interactions.

B Spin-stand and centrifuge vision system

As shown in Fig. 5, the CD spin-stand is equipped with a motor (Pacific Scientific Servo Motor) and an amplifier/controller (PAC SCI Programmable Servo Drive) which enables various rotational profiles and precise positioning. The servo drive uses a graphical user interface program, ToolPAC, to easily

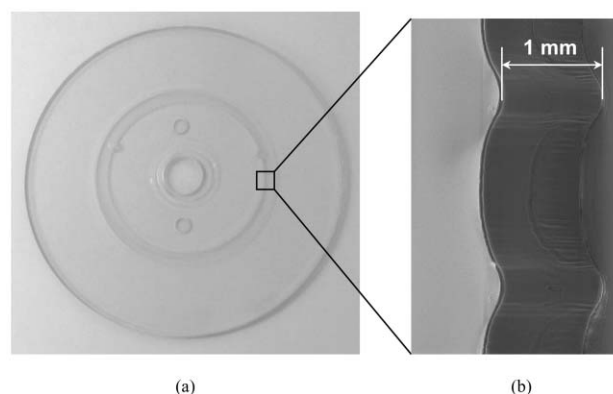


Fig. 4 The CD designed for cell lysing (a) CD with an annular chamber (total volume of 1 mL) (b) SEM photo of a wavy inner wall of the chamber.

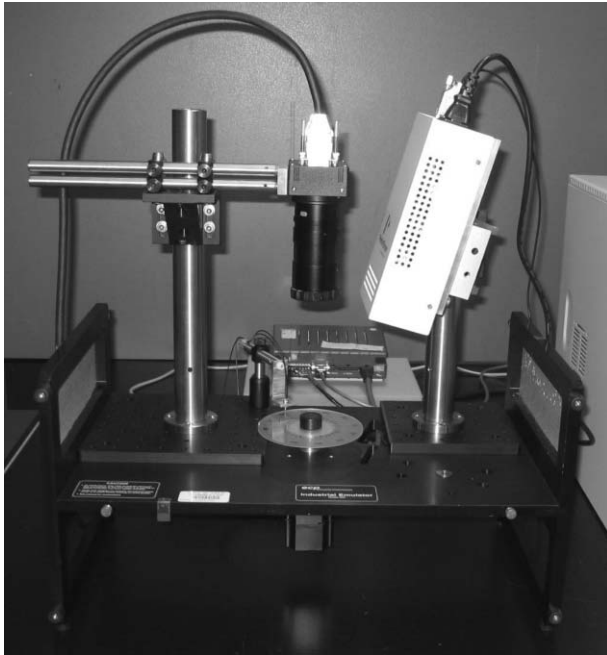


Fig. 5 The spin-stand and centrifuge vision system.

configure and program the motor for specific applications. A microfluidic CD to be tested is placed on an aluminium platen coupled to the motor shaft and is locked in place by a black plastic screw.

With a centrifuge vision system, one can view a sequence of color images of the area of interest on the CD in real time (while it is rotating) and store the captured frames on a computer. The digital video recording system is composed of: a camera (Basler A301bc, 640×480 pixels, 80 fps max., $10\times$ zoom lens mounted), a strobe light (PerkinElmer MVS-4200, 6 μ s duration), and a retro-reflective fiber optic sensor (Banner D10 Expert Fiber-Optic Sensor). The strobe light, with a 100 Hz maximum repetition frequency, is employed to reduce blurry images of a fast moving object. In order to generate synchronized signals, a white square mark (2 mm \times 2 mm) is placed on the surface of the CD and is aligned such that it falls immediately below the light spot emitted from the fiber optic sensor. Thus whenever this square comes under the light beam of the sensor, a pulse will be sent to the video capture board which will then immediately trigger the camera and strobe light to grab one image frame per revolution.

C. Procedure for inducing rimming flow

Periodic granular rimming flow is induced in a partially filled annular lysing chamber by spinning the CD around a horizontal axis with high acceleration (e.g., 1000 rev s^{-2}) and alternating rotational directions with a tiny rest period in between (e.g., 150 ms) to accumulate a solid-liquid mixture at the bottom of the chamber (see Fig. 7(a)). The CD makes 15 or 20 complete revolutions depending on the chosen angular velocity (e.g., $50\text{--}100 \text{ rev s}^{-1}$) and then returns to its original position with the same angular velocity and the same number of revolutions—a typical spin cycle profile is shown in Fig. 6. The CD then runs for hundreds of such cycles to ensure that a large number of effective particle impacts occur. The angular acceleration rate is so high that a circumferential particle band begins to be observed after one complete revolution corresponding to about 0.05 s. In Fig. 7 we show a sequence of flow patterns to illustrate how a solid-liquid mixture develops into a rimming flow.

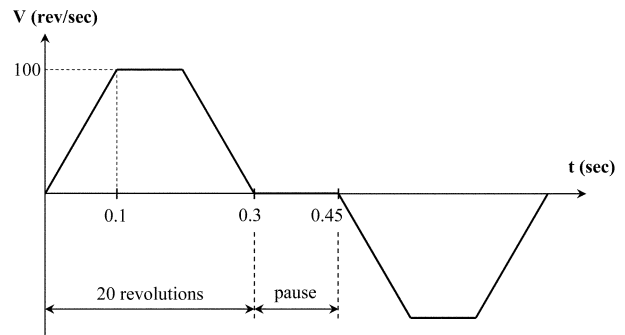


Fig. 6 The rotational profile for a spin cycle: A CD spinning up to 100 rev s^{-1} with an acceleration of 1000 rev s^{-2} makes 20 revolutions and spins back to its original position with a pause between the alternations.

D. Cell strains and culture conditions

Chinese Hamster Ovary cell line CHO-K1 (Clontech, CA) was used as a model cell line for mammalian cell lysis. The cells were cultivated in a Dulbecco's Modified Eagle's Medium (Sigma), supplemented with 3.7 g L^{-1} sodium bicarbonate (Sigma), 40 mg L^{-1} L-glutamine (Sigma) and 20% of a fetal bovine serum (Clontech, 8630-1) in the presence of 100 mg L^{-1} G418 (Gibco), 100,000 units per liter penicillin (Sigma) and 100 mg L^{-1} streptomycin sulfate (Sigma) at 37°C , 5% carbon dioxide. The cells were inoculated from vials stored in a -80°C freezer into 10 cm tissue culture plates (Fisher Scientific). The cells were then detached by 0.25% trypsin in 0.5 mM EDTA and resuspended in Dulbecco's phosphate buffered saline solution (Sigma). The cell density was approximately 100,000 cells per mL.

Saccharomyces cerevisiae. Strain TMy16 (*MATa trp1- Δ 901 ura3-52 his3- Δ 201 ade2-101 lys2-1 leu1-12 can1-100 GAL⁺*)²⁵ and *Escherichia coli* strain XL1-Blue (Stratagene, CA) containing plasmid pDUB²⁶ were used for yeast and bacterial cell lysis. Nonselective YPD medium²⁷ was used for cultivating *S. cerevisiae* and LB medium¹⁰ containing 50 mg L^{-1} ampicillin sodium salt was the *E. coli* nutrient medium. Batch cultures of both yeast and bacteria were grown in 16 mm \times 125 mm

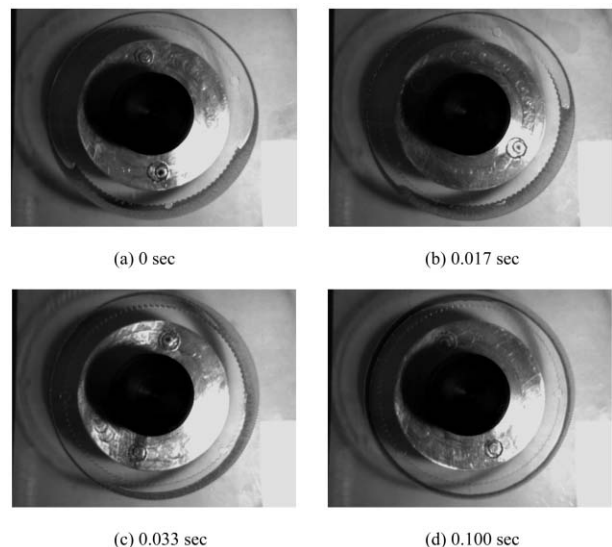


Fig. 7 Sequential images of the flow for a mixture of zirconia-silica beads and blue-dyed liquid (for contrast) forming circumferential bands (rimming flow) upon rotation: a solid volume fraction of 0.25 and angular velocity of 100 rev s^{-1} . The images are captured at a frame acquisition rate of 60 Hz.

culture tubes (Fisher Scientific) containing 5 mL medium. Seed cultures were inoculated from vials stored in a -80°C freezer and incubated in an air shaker (New Brunswick, model G25) at 250 rpm and 30°C , 2 days for yeast and 37°C , overnight for bacteria. Subsequent tubes were inoculated (1% v/v) and incubated in an air shaker (New Brunswick, model G25) at 250 rpm and 30°C for yeast and 37°C for bacteria. The cell concentration was measured at OD_{600} with a spectrophotometer (Novaspec II, Phamacia).

E. Traditional protocol for yeast lysis

A traditional glass bead yeast cell lysis protocol²⁸ was utilized for comparison with our CD-based lysis method. A volume of 0.3 mL of yeast cells ($\text{OD}_{600} = 2.0$) was transferred to a microcentrifuge tube and centrifuged for 1 min to pellet the cells. The supernatant was discarded and 200 μL of lysis buffer (1% SDS, 1 mM EDTA, 100 mM NaCl, 10 mM Tris (pH 8), 2% Triton X-100), 200 μL phenol-chloroform:isoamyl alcohol (Sigma) and 0.3 g of 425–600 μm glass beads (Sigma, G-8772) were added. Using a vortex (Fisher Scientific) placed in the refrigerator, we vortexed the microtube for 5 min. After vortexing we added 200 μL of water, briefly mixed manually, centrifuged the tube for 10 more min and finally transferred the top aqueous layer to a new microcentrifuge tube to be analyzed.

F. Cell microscopy and measurement of DNA concentration

CHO-K1 cells were observed using a microscope (Nikon, TE300) and photographed (Roper Scientific, Photometrics Cool Snap) before and after spinning the CD to verify the cell disruption. For *E. coli* and yeast, the amount of DNA present after cell lysis was measured using the PicoGreen Quantitation Kit (Molecular probes, OR); this assay exploits the affinity of the PicoGreen reagent for double stranded DNA and its fluorescence intensity dependence on the dsDNA concentration. The samples were excited at 480 nm and the fluorescence emission intensity measured at 520 nm using a Luminescence Spectrometer (Research Instruments, Aminco Bowman Series 2). The DNA concentration of each sample was extrapolated from a standard curve of fluorescence emission intensity versus DNA concentration.

IV Experimental results and discussion

A Mammalian cells (CHO-K1)

A volume of 0.3 mL (approximately 100,000 cells per ml) of Chinese Hamster Ovary (CHO-K1) cells was loaded into a lysis chamber along with 0.25 g of acid-washed glass beads (density of 2.5 g cc^{-1}). Two sizes of glass beads were used, the first was approximately 106 μm in diameter (Sigma, G-4649) and the second ranged from 150 to 212 μm (Sigma, G-1145). The two types of beads were mixed in a 7:3 ratio, respectively. A mixture of medium and beads approximately filled the lysis chamber halfway with a solid volume fraction of 0.25. The CD was then spun up to 50 rev s^{-1} for a period of 300 cycles. Mammalian cells are, in general, easy to disrupt and thus are not the optimal choice to test the important parameters for lysis discussed before. Therefore, we only checked mammalian cell lysing using simple microscopy. A microscope view before and after spinning the CD in Fig. 8 shows that almost all of the cells were lysed leaving a large amount of cell debris.

B Bacterial cells (*Escherichia coli*)

For the *E. coli* lysis tests, the same glass beads used in the mammalian test were exploited to study the effect of solid volume fractions (SVF) on lysis efficiency. The cell concentration was set to an optical density ($\text{OD}_{600} = 2.0$). The two sizes

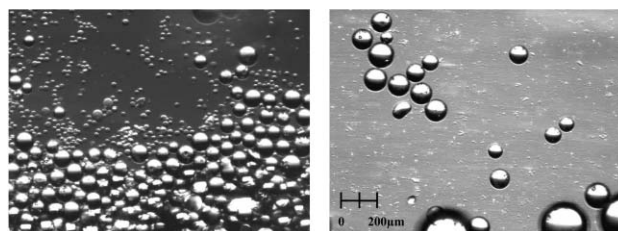


Fig. 8 Comparison of mammalian cells before (left) and after (right) spinning the CD. The large spheres are glass beads and the small semicircular spots ($\sim 10\ \mu\text{m}$) on the left are CHO-K1 cells. The image on the right shows cell debris from the lysis of the CHO-K1 cells.

of glass beads were mixed at the same ratio of 7:3. The total volume of the mixture was fixed at 0.45 mL for each volumetric ratio of cell suspension to beads of 2:1, 3:1, and 4:1. A CD was ramped up to 75 rev s^{-1} for a period of 600 cycles. As shown in Fig. 9, a higher solid volume fraction resulted in a larger amount of DNA extracted (and thus a larger number of cells lysed), reaching a maximum at a ratio of 2:1.

In fact, additional tests were performed to find a peak in SVF. Above the 2:1 ratio, the bulk of accumulated beads at the bottom of the chamber just rotated around the axis along with the disc and such a flow (*i.e.*, non-rimming flow) did not contribute any further to lysing. Accordingly, the 2:1 ratio was a practical limit at which we could ensure the rimming flow formation in the current experimental setup and thus was concluded to be a peak in SVF. We also tested a control CD containing the cell suspension (0.45 mL) without beads to determine the contribution of the beads to the lysing process and verified that in this case very little DNA was extracted by comparing the fluorescence intensity of the suspension before and after spinning.

The test 1, 2, and 3 were performed on different days but the cell concentration for each test was always adjusted to a constant optical density (*i.e.*, $\text{OD}_{600} = 2.0$). Nevertheless, we observed large variations in the measured DNA concentration as shown in Figs. 9, 10(a), and 10(b). The reason is simple; although this type of cell quantification is popular in biology research labs, it is not a very accurate method. Another reason may be found in the medium used for cultivating cells. As a new medium was prepared and used to grow cells for each test, the slight differences among the media may affect the cell conditions and thus cause variation in lysing capacity.

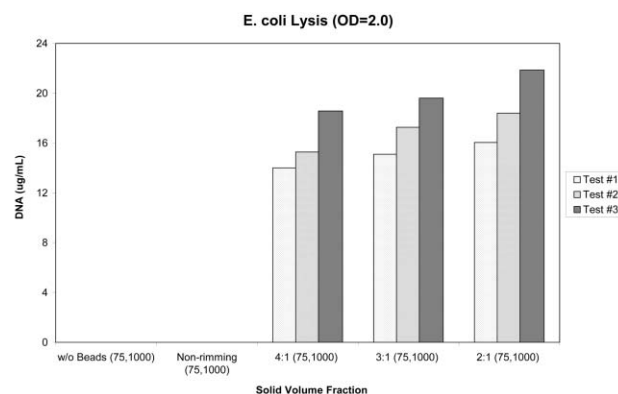


Fig. 9 A plot of dsDNA concentrations of *E. coli* lysis vs. the volumetric ratios of cell suspension to glass beads (without beads, non-rimming, 4:1, 3:1, and 2:1). The numbers separated by a comma in parenthesis are angular velocity (rev s^{-1}) and acceleration rate (rev s^{-2}). All CDs were spun for a period of 600 cycles. The concentrations for each volumetric ratio were extrapolated from a standard dsDNA calibration curve. The test 1, 2, and 3 were performed on different days with the cell concentration adjusted to a constant optical density ($\text{OD}_{600} = 2.0$).

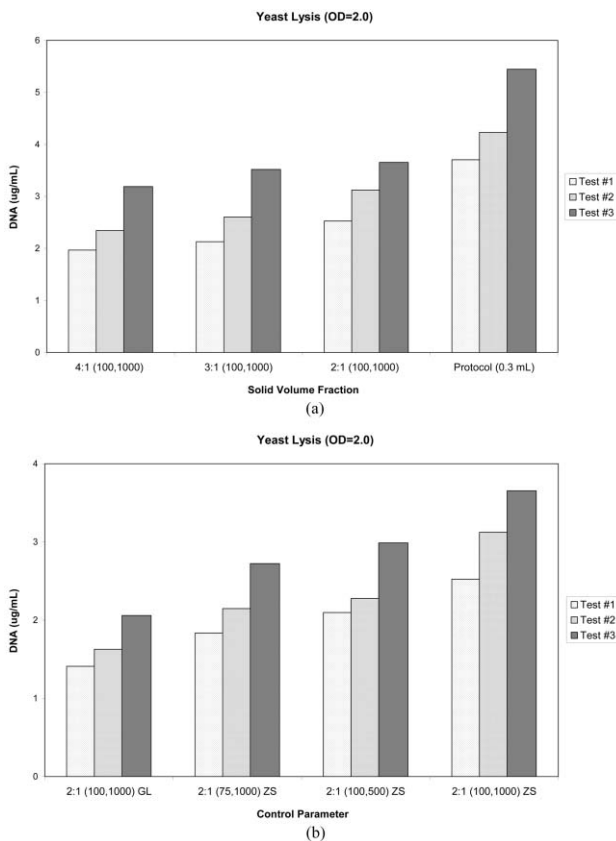


Fig. 10 Plots of dsDNA concentrations of yeast lysis (a) vs. the volumetric ratios of cell suspension to zirconia–silica beads and a common lysis protocol (b) vs. the control parameters (from left): bead density, angular velocity, and acceleration rate (the fourth grouped columns as a reference). GL and ZS stand for glass beads and zirconia–silica beads, respectively and are of the same size range (150–250 μm). The numbers separated by a comma in parenthesis are angular velocity (rev s^{-1}) and acceleration rate (rev s^{-2}). All CDs were spun for a period of 500 cycles. The test 1, 2, and 3 were also performed on different days with the cell concentration adjusted to a constant optical density ($\text{OD}_{600} = 2.0$).

C Yeast cells (*Saccharomyces cerevisiae*)

Yeast constitutes the hardest cell to disrupt among our choice of cells and was tested for all specified control parameters to determine the contribution of each (except for particle size). The cell concentration was fixed to give a constant optical density ($\text{OD}_{600} = 2.0$). For SVF test, zirconia–silica beads (density of 3.7 g cc^{-1}) with a particle size ranging from 150 to 250 μm were employed at an angular velocity of 100 rev s^{-1} for a period of 500 cycles. As shown in Fig. 10(a), the amount of extracted dsDNA increases with higher solid volume fraction, reaching a peak at 2:1 ratio—the same trend we observed in the *E. coli* tests. Additional yeast tests with the 2:1 ratio were performed while varying other parameters such as acceleration rate, angular velocity, and the density of beads (see Fig. 10(b)). From these test sets, the control parameters were compared, in terms of dsDNA concentration extracted from lysis, to find the factors contributing the most to cell lysis efficiency. The use of different beads but of the same size (e.g., glass beads vs. zirconia–silica beads) resulted in the largest lysis yield relative to parameter change followed by the angular velocity. Therefore, the bead density was concluded to be the most contributing parameter to cell lysing within the given range of the parameters. On the other hand, we admit that it is not straightforward to determine the true influence of angular velocity purely based on the numerical result because the actual impact velocity would be slower than the terminal settling

velocity in eqn. (6) due to the fact that a majority of particle impacts may occur within acceleration periods and thus the particles could not fully develop to their terminal settling velocities for an intended angular velocity.

A common yeast lysis method (see above) used in biological laboratories was also compared with our model, and our optimally configured setup showed approximately 65% of the efficiency of the traditional yeast lysis method in Fig. 10(a). Of course, our method is purely mechanical and therefore simpler to implement in a miniaturized platform whereas the traditional method is both mechanical and chemical.

V Conclusions

We have investigated a mechanical method for rapid cell lysis in the rimming flow established inside a partially solid–liquid mixture-filled annular chamber in a microfluidic CD which rotates around a horizontal axis of rotation. Two types of inter-particle forces (friction and collision) are at play. These forces simultaneously apply to enhance the disruption of biological cells in the rapid granular shear flow.

Our experiments identified the relative contribution of control parameters such as bead density, angular velocity, acceleration rate, and solid volume fraction. We concluded that the most important parameter among them was the bead density closely followed by the angular velocity in the present CD design. In addition, the experiments also demonstrated the dependence of lysis yield on the acceleration rate of the disc, indicating that higher acceleration rate leads to a larger magnitude of frictional contact of particles. For higher particle concentrations, more cells were disrupted due to larger inter-particle forces as well as increased number of effective impacts. In the SVF tests, a SVF of 0.33 (i.e., 2:1 ratio) was found to be a peak for the maximum lysis efficiency since the rimming flow was hardly observed beyond it. Moreover, compared to a yeast lysis method frequently used in biological laboratories, our novel design demonstrated a little lower lysis capability without the use of any chemical lysis agent.

We conclude this paper with a brief comment that our experiments successfully demonstrated cell lysis on a CD platform through a mechanical method, and this work will be an integral part for our long-term goal—an automated CD-based sample preparation and nucleic acid testing platform.

Acknowledgement

We would like to thank Dr Seog Woo Rhee in the Department of Biomedical Engineering at UC, Irvine for taking microscopic images of mammalian cells in CD.

References

- 1 M. J. Madou, *Fundamentals of Microfabrication*, CRC Press, Boca Raton, FL, 2nd edn., 2002.
- 2 G. T. A. Kovacs, *Micromachined Transducers Sourcebook*, McGraw-Hill, NY, 1998.
- 3 A. Manz, C. S. Effenhauser, N. Burggraf, D. J. Harrison, K. Seiler and K. Fluri, *J. Micromech. Microeng.*, 1994, **4**, 257–265.
- 4 M. G. Pollack, A. D. Shenderov and R. B. Fair, *Lab Chip*, 2002, **2**, 96–101.
- 5 M. J. Madou, L. J. Lee, S. Daunert, S. Lai and C.-H. Shih, *Biomed. Microdevices*, 2001, **3**(3), 245–254. ★ This paper highlights several crucial microfluidic functions that can be integrated on CD platform for biomedical diagnostics.
- 6 M. J. Madou and G. J. Kellogg, *Proc. SPIE*, 1998, **3259**, 80–93.
- 7 T. Brenner, T. Glatzel, R. Zengerle and J. Ducee, *Proc. μTAS 2003*, Lake Tahoe, USA.
- 8 D. Di Carlo, K.-H. Jeong and L. P. Lee, *Lab Chip*, 2003, **3**, 287–291. ★ This paper demonstrates reagentless mechanical cell lysis by nanoscale barbs in microfluidic channels.

-
- 9 S.-W. Lee and Y.-C. Tai, *Sens. Actuators, A*, 1999, **73**, 74–79.
 - 10 J. Sambrook and D. W. Russell, *Molecular Cloning*, CSHL Press, Cold Spring Harbor, NY, 2001.
 - 11 A. Q. Shen, *Phys. Fluids*, 2002, **14**(2), 462–470.
 - 12 P. Jalali, M. Li, J. Ritvanen and P. Sarkomaa, *Chaos*, 2003, **13**(2), 434–443.
 - 13 K. J. Ruschak and L. E. Scriven, *J. Fluid Mech.*, 1976, **76**, 113–127.
 - 14 S. T. Thoroddsen and L. Mahadevan, *Exp. Fluids*, 1997, **23**, 1–13.
 - 15 R. A. Bagnold, *Proc. R. Soc. London, Ser. A*, 1954, **225**(1160), 49–63.
 - 16 C. K. K. Lun, *Phys. Fluids*, 1996, **8**(11), 2868–2883.
 - 17 S. F. Foerster, M. Y. Louge, H. Chang and K. Allia, *Phy. Fluids*, 1994, **6**(3), 1108–1115.
 - 18 G. K. Batchelor, *J. Fluid Mech.*, 1988, **193**, 75–110.
 - 19 R. Zenit, M. L. Hunt and C. E. Brennen, *J. Fluid Mech.*, 1997, **353**, 261–283.
 - 20 Frank M. White, *Fluid Mechanics*, McGraw Hill, 5th edn., 2002.
 - 21 S. A. Morsi and A. J. Alexander, *J. Fluid Mech.*, 1972, **55**, 193–208.
 - 22 G. M. Whitesides, E. Ostuni, S. Takayama, X. Jiang and D. E. Ingber, *Annu. Rev. Biomed. Eng.*, 2001, **3**, 335–373.
 - 23 H. Lorenz, M. Despont, N. Fahrni, J. Brugger, P. Vettiger and P. Renaud, *Sens. Actuators, A*, 1998, **64**, 33–39.
 - 24 http://www.microchem.com/products/pdf/SU8_50-100.pdf.
 - 25 J. Kirchner and S. Sandmeyer, *J. Virol.*, 1993, **67**, 19–28.
 - 26 F. W. Lee and N. A. DaSilva, *Biotechnol. Prog.*, 1997, **13**, 368–373.
 - 27 F. Sherman, G. R. Fink and J. B. Hicks, *Methods in Yeast Genetics*, CSHL Press, Cold Spring Harbor, NY, 1986.
 - 28 M. H. Nymark-McMahon, N. S. Beliakova-Bethell, J.-L. Darlix, S. F. J. Le Grice and S. B. Sandmeyer, *J. Virol.*, 2002, **76**(6), 2804–2816.